ORIGINAL RESEARCH

Decreased *Porphyromonas gingivalis* adhesion and improved biocompatibility on tetracycline-loaded TiO$_2$ nanotubes: an in vitro study

Lei Sun[1]
Jiliang Xu[1]
Zihuan Sun[1]
Fang Zheng[2]
Chun Liu[1]
Chao Wang[1]
Xiaoye Hu[3]
Lunguo Xia[4]
Zhou Liu[5]
Rong Xia[1]

[1]Department of Stomatology, The Second Affiliated Hospital of Anhui Medical University, Hefei, Anhui, People's Republic of China; [2]Department of Mathematics, University of Science and Technology of China, Hefei, Anhui, People's Republic of China; [3]Key Laboratory of Materials Physics, Anhui Key Laboratory of Nanomaterials and Nanotechnology, Institute of Solid State Physics, Chinese Academy of Sciences, Hefei, Anhui, People's Republic of China; [4]Department of Orthodontics, Collage of Stomatology, Ninth People's Hospital, School of Medicine, Shanghai Jiao Tong University, Shanghai, People's Republic of China; [5]Department of Laboratory Medicine, The Second Affiliated Hospital of Anhui Medical University, Hefei, Anhui, People's Republic of China

Correspondence: Rong Xia
Department of Stomatology, The Second Affiliated Hospital of Anhui Medical University, 678 Furong Road, Hefei 230032, Anhui, People's Republic of China
Tel +86 5 516 386 9415
Fax +86 5 516 386 9400
Email xiarongah@hotmail.com

Background: Titanium dioxide (TiO$_2$) nanotubes are often used as carriers for loading materials such as drugs, proteins, and growth factors.

Materials and methods: In this study, we loaded tetracycline onto TiO$_2$ nanotubes to demonstrate its antibacterial properties and biocompatibility. The two-layered anodic TiO$_2$ nanotubes with a honeycomb-like porous structure were fabricated by using a two-step anodization, and they were loaded with tetracycline by using a simplified lyophilization method and vacuum drying. Their physical properties, such as chemical compositions, wettability, and surface morphologies of the different samples, were observed and measured by X-ray photoelectron spectroscopy (XPS), contact angle measurement, and scanning electron microscopy (SEM). The in vitro growth behaviors of mouse bone marrow stromal cells (BMSCs) on these substrates were investigated.

Results: The TiO$_2$ nanotube (NT) substrates and the tetracycline-loaded TiO$_2$ nanotube (NT-T) substrates revealed a crucial potential for promoting the adhesion, proliferation, and differentiation of BMSCs. Similarly, the NT-T substrates displayed a sudden release of tetracycline in the first 15 minutes of their administration, and the release tended to be stable 90 minutes later. The antibacterial performances of the prepared substrates were assessed with *Porphyromonas gingivalis*. The result showed that NT and NT-T substrates had antibacterial capacities.

Conclusion: Overall, this research provides a promising method with potential for clinical translation by allowing local slow release of antimicrobial compounds by loading them onto constructed nanotubes.

Keywords: *Porphyromonas gingivalis*, tetracycline, TiO$_2$ nanotubes, mouse bone marrow stromal cells, antibacterial, drug release

Introduction

Pure titanium (PT) and its alloys are widely used in implant materials in the dental and orthopedic fields on account of their good biocompatibility and their high resistance to corrosion.[1,2] Dental implants have been applied for more than 30 years to reconstruct the masticatory function or for esthetic concerns associated with missing teeth.[3] Meanwhile, titanium-based surfaces can provide favorable conditions for bacterial adhesion and biofilm formation.[4] Bacterial colonization and biofilm formation may lead to increased occurrences of infection,[5,6] such as peri-implantitis, which is a common occurrence. Peri-implantitis is an inflammatory disease that originates from infection and ultimately results in the loss of the alveolar bone that contacts implants.[7–10] It is caused by biofilms formed around the implant. During biofilm formation, *Porphyromonas gingivalis* is regarded as the primary pathogen that comprises these biofilms, which is involved in the initiation and progression of severe forms of peri-implantitis.[11,12] Therefore,

effective control of the adhesion and growth of pathogenic *P. gingivalis* is crucial for inhibiting or treating peri-implantitis and improving the success rate of dental implants.

Systemic antibiotic treatment, such as perioperative antibiotic prophylaxis, is a routine procedure used to prevent postsurgical infection.[13] However, it may also give rise to many relevant complications ranging from diarrhea to life-threatening allergic reactions. Moreover, the emergence of antibiotic-resistant bacteria is another major concern relating to the widespread use of antibiotics.[14–16] Hence, it is necessary and important to prevent implant-related infection by improving surface antibacterial properties and to develop methods to deliver antibiotics topically around dental implants that could resolve the problem and maintain adequate concentrations of antibiotics around the implant.

Titania nanotubes can be fabricated regularly with nanotopographical features by electrochemical anodization. Titania nanotubes can provide abundant space to improve osteogenic activity and can act as carriers for drug delivery.[17–19] A previous study showed that nanotubes can exhibit moderate antibacterial ability.[17] Tetracycline (TET), a broad-spectrum antibiotic, can inhibit gram-negative and some gram-positive pathogens.[20] These pathogens can cause implant-related infections such as peri-implantitis. Nanotubes loaded with TET can deliver high levels of antibiotics locally to control bacterial colonization around the implant without causing systemic toxicity; simultaneously, these nanotubes would not change the osseointegrative properties of the surface.

In this work, a titanium surface coated with double layers of nanotubes was fabricated using the two-step electrochemical anodic oxidation method. The biocompatibility of double-layered titania nanotube arrays has already been verified in previous studies. The surfaces of double-layered titania nanotubes promoted adhesion, proliferation, and differentiation of mouse bone marrow stromal cells (BMSCs).

In this article, contact angle, XPS, and SEM measurements were used to analyze the contact angle of the surface of the TET-loaded titania nanotubes to the chemical elements and the microstructure. The ability to inhibit antibiotic release from the nanotubes was analyzed. Osteogenic activity and antibacterial ability (against *P. gingivalis*) of TET-loaded and nonloaded double-layered titania nanotubes were investigated and compared.

Materials and methods
Fabrication of two-layered honeycomb-like porous anodic TiO$_2$ nanotubes

Two-layered anodic titanium dioxide (TiO$_2$) nanotubes with a honeycomb-like porous structure were fabricated by two-step anodization of PT foil (99.99%). Prior to the electrochemical anodization treatment, PT foils (12 mm in diameter and 0.25 mm in thickness) were polished step-by-step using metallographic sandpaper (from 800 # to 7,000 #) to achieve a mirror effect and then were sonicated with acetone, ethyl alcohol, and deionized water. The electrolyte concentration was 88 mmol/L ammonium fluoride in ethylene glycol. In the first step, PT foils were anodized under a voltage of 60 V for 2.5 hours at room temperature to form large-sized TiO$_2$ nanotube arrays. Then, the titanium foils were processed in deionized water using ultrasonic processing to remove the as-formed TiO$_2$ nanotube arrays. Regularly arranged TiO$_2$ nanocell arrays with shallow bowl shapes that were remaining on the titanium foil were obtained. In the second step, the remaining titanium foils were anodized again under a voltage of 12 V for 40 minutes to form small nanopores below each shallow, bowl-shaped honeycomb cell. We found that the diameter of the top shallow, bowl-shaped cells increased so that the bowl-shaped cells changed into a honeycomb shape. These prepared titanium foils were sonicated with deionized water and then dried in the ambient atmosphere, and the foils were denoted as "NT." More details on the above fabrication of similar two-layered anodic TiO$_2$ nanotubes are further described elsewhere.[21]

TET loading

TET was loaded into the TiO$_2$ nanotubes by a simplified lyophilization method followed by vacuum drying according to previous reports.[22,23] Briefly, the NT surfaces were cleaned with deionized water before loading. A TET solution (Sangon Biotech) of 50 mg/mL was prepared in PBS. A volume of 20 μL of the TET solution was pipetted onto the nanotube surfaces and gently spread to ensure even coverage. The surfaces were dried using a vacuum for 20 minutes at room temperature. After drying, the abovementioned loading step was repeated until the nanotubes were loaded with 60 μg of TET. After the last drying step, the sample surfaces were quickly washed by pipetting 500 μL of PBS to remove any excess drug ingredients. The washed solutions were collected and stored for further analysis. The titanium foils were then dried in an ambient atmosphere, and these foils were denoted as "NT-T."

Surface characterization

The surface morphology was viewed by SEM (Sirion-200, FEI, Hillsboro, OR, USA). The chemical states and chemical compositions of the specimen surfaces were investigated by XPS (ESCALAB 250, Thermo Scientific, Waltham, MA, USA).

Contact angle measurement

After 1 μL of deionized water was gently dropped onto the surface of these specimens, the water contact angle was

measured with a pendant drop method using a contact angle meter (SL200B, Solon Technology Co., Shanghai, China) at room temperature.

Drug release evaluation

To measure how TET was released from the two-layered nanotubes, the sample surfaces were immersed into 500 mL of PBS in a 24-well plate while it was subjected to orbital shaking at 70 rpm at room temperature. A 200 µL sample of the solution was taken from the 24-well plate at 15-minute intervals to ascertain the release kinetics of TET. In the meantime, 200 mL of fresh PBS was added into the plate to keep the total amount solution unchanged at 500 mL. Samples of this solution were collected regularly for up to 120 minutes. The samples of this solution were analyzed for drug content using a HPLC system (LC-20AD, SHIMADZU Co., Kyoto, Japan). A standard curve with known concentrations of TET was used to ascertain the unknown concentrations.

Bacterial culture

P. gingivalis (ATCC 33277) was used in this study. These strains were stored at −80°C in glycerol stock and were propagated overnight in brain-heart infusion (BHI) sheep blood solid medium. All cultures were incubated under anaerobic conditions at 37°C. A sterile 10 µL loop was used to withdraw bacteria colonies from the BHI solid medium, which were then inoculated into 10 mL of BHI broth and cultured overnight. Samples of NT, PT, and PT-T were sterilized for 2 hours at 55°C with ethylene oxide.

Bacterial adhesion experiment using the spread plate method

Antibacterial activity of PT and PT-T samples was tested in *P. gingivalis* using a bacterial adhesion test that was quantified by counting colony-forming units (CFUs). The inoculum of each strain was prepared by regulating the concentration of an overnight bacterial culture to a turbidity equal to a 0.5 McFarland standard in BHI broth.

Confined in a laminar flow hood, samples were put into sterile petri dishes. A 20 µL volume of the *P. gingivalis* suspension was pipetted onto the sample surface with the cover glass coated to spread the liquid, where it evenly covered the surface of the specimen and was incubated under a lid at 37°C for 3 hours under anaerobic conditions. Petri dishes were filled with wet cotton balls to encourage an appropriate level of humidity to ensure that suspension liquid evaporation was kept to a minimum. Then, the samples were removed with sterile forceps and carefully washed with 5 mL sterile PBS three times to remove loosely adherent bacteria. The samples

were then placed into fresh centrifuge tubes that contained 5 mL of fresh PBS, and the bacteria that were adherent onto the disc were dislodged by using a whirlpool mixer (XH-B, Medical Apparatus Co., Ltd, Jiangsu, China) at its maximum power for 5 minutes. This method has been shown to allow the removal of biomaterial-adherent bacteria.[24,25] A 100 µL volume of the vortexed solutions was coated evenly in triplicate onto BHI sheep blood solid medium and then incubated for 48 hours at 37°C. The number of CFUs on the BHI medium was counted.

The antibacterial ratio was counted by using the following formula: $(A-B)/A \times 100\%$, where A is the average number of bacteria in the PT specimen (CFU/specimen), B is the average number of bacteria in the NT and NT-T specimens (CFU/specimen).

Bacterial adhesion assessed using SEM

The bacterial culture was as described above. Bacteria were incubated under a lid at 37°C for 3 hours in anaerobic conditions. After this incubation, the surfaces were fixed with 2.5% glutaraldehyde for 2 hours and were washed with sterile PBS. The samples were subjected to a gradient dehydration in ethanol: 25%, 50%, 75%, 95%, and 100% ethanol concentrations for 10 minutes each. The surfaces were then air-dried for 30 minutes. The surfaces of the specimens were then treated with gold spray and observed using SEM.

Bacterial adhesion assessed using fluorescence microscopy

The inoculum for each of the strains was prepared by adjusting the concentration of an overnight bacterial culture to a turbidity equal to a 2 McFarland standard in BHI broth. Confined in a laminar flow hood, samples were put into sterile petri dishes. A 20 µL volume of the *P. gingivalis* suspension was pipetted onto the samples' surfaces with the cover glass coated to spread the bacteria liquid to evenly cover the surface of the specimen and were incubated under a lid at 37°C for 3 hours under anaerobic conditions. Petri dishes were filled with a wet cotton ball to control the level of humidity and ensure that suspension liquid evaporation was kept to a minimum. Afterward, the samples were removed with sterile forceps and were carefully washed three times with 5 mL of sterile PBS to remove loosely adherent bacteria. The samples were placed into fresh centrifuge tubes with 5 mL of fresh PBS, and the adherent bacteria on the disc were dislodged by using a whirlpool mixer at maximum power for 5 minutes. DAPI (Beyotime Biotech, Jiangsu, China) staining solution was added to the vortexed solutions on glass slide for 5 minutes. After washing with PBS three

times with a 3-minute interval, slides were covered with 50% glycerol in water. Fluorescence images were captured using a fluorescence microscope (BX53, OLYMPUS Corporation, Tokyo, Japan).

Cell adhesion

The mouse BMSCs were purchased from Cyagen Biotech Company. The cells were cultured in stem cell complete culture medium and were used within five passages in this study.

PT, NT, and NT-T were randomly chosen and were placed in 24-well plates. The cells were seeded at a density of 5×10^4/well. The discs were first incubated for 120 minutes at 37°C in an incubator and were then carefully washed three times with PBS followed by 2.5% glutaraldehyde fixation for 24 hours. Their surfaces were then air-dried for 30 minutes. The specimens were then sputter coated with gold and inspected utilizing SEM.

Cell proliferation

PT, NT, and NT-T were randomly chosen and were placed in 24-well plates. Then, BMSCs were seeded at a density of 1×10^4/well. After culturing for 1, 3, and 5 days, cell proliferation in the samples was assessed using the MTT assay. Cells were carefully washed with PBS three times at each time point, and then 200 µL of the MTT solution (5 mg/mL) and 800 µL of DMEM without serum and phenol red were added into each sample. The samples were incubated for 4 hours at 37°C, the supernatant was removed, and 1 mL DMSO was put into each well. The absorbance of the solution was analyzed using a spectrophotometer at 490 nm.

Cell differentiation

PT, NT, and NT-T were randomly chosen and were put in 24-well plates. Then, BMSCs were seeded at a density of 1×10^5/well. After culturing for 3, 5, and 7 days, 0.2%

Triton X-100 solution was used to lyse cells for 30 minutes. Then, the lysis solution was treated with an ALP staining kit (Nanjing Jiancheng Bioengineering Institute, Nanjing, China).

Statistical analysis

The results are expressed as the means ± SD with all groups conducted in triplicate. The one-way ANOVA and least significant difference post hoc tests were used for statistical analysis, where $P<0.05$ was considered significant and $P<0.01$ was considered highly significant.

Results and discussion
Surface appearances

SEM, XPS, and a contact angle meter were used to investigate the surface physicochemical properties of PT, NT, and NT-T samples. PT sheets were polished by a physical treatment that showed a relatively rough surface morphology with visible scratches (Figure 1A).[26] Nanoporous titanium was prepared onto PT substrates by using an anodization approach.[27] As previous studies have reported, anodic oxidation is a controlled and cost-effective technology to form TiO_2 nanoscale structures with tunable morphology that is achieved by adjusting voltage and electrolyte concentrations relating to the procedure.[28,29] Figure 1B shows the SEM images of two layers of the cellular TiO_2 nanotube array. From the superior aspect, the sample was divided into a large amount of homogeneous hexagonal nanoscale cells that each had a diameter of approximately 160 nm, and there were approximately 50 nanopores with a diameter approximately 15 nm in each hexagonal cell. The specific description can be observed in our previous work.[21] After TET was loaded onto the NT surface, the intersmall nanotube diameter was narrowed and outer large nanotubes were partially blocked (Figure 1C). This suggests that TET-deposited TiO_2 nanotubes arrays were partially covered.
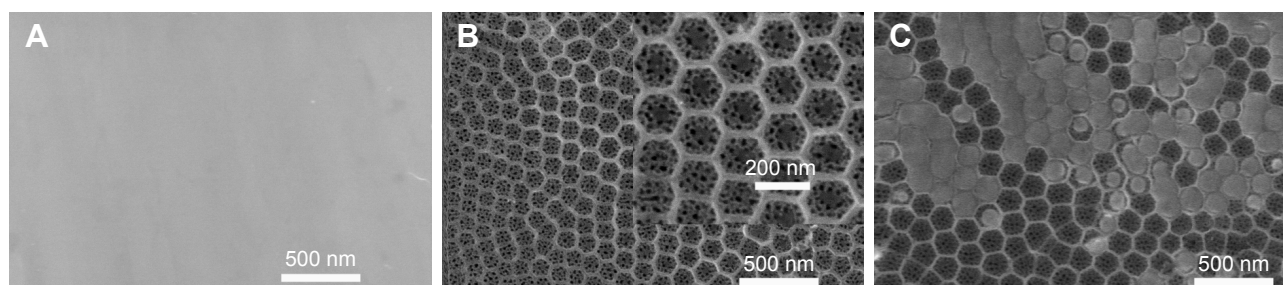

Figure 1 SEM images of the surface morphologies of different substrates: (**A**) PT, (**B**) NT, and (**C**) NT-T.
Note: Inserted images display the observed morphologies at high magnification.
Abbreviations: NT, nanotubes; NT-T, tetracycline-loaded nanotubes; PT, pure titanium; SEM, scanning electron microscopy.

Table 1 The chemical compositions of the PT, NT, and NT-T substrates by XPS

%	Ti	O	C	N
PT	15.12	52.79	30.36	1.72
NT	19.41	50.54	19.84	0.84
NT-T	1.24	25.79	65.81	5.55

Abbreviations: NT, nanotubes; NT-T, tetracycline-loaded nanotubes; PT, pure titanium; XPS, X-ray photoelectron spectroscopy.

Each chemical composition analysis of PT, NT, and NT-T samples was characterized by XPS (Table 1 and Figure 2). Approximately 15.12% of Ti, 52.79% of O, 30.36% of C, and 1.72% of N (atomic concentration) were detected in a PT sample. As previously reported,[30–32] elemental carbon on the surface of PT may be due to the physical adhesion of hydrocarbons from the surrounding environment, which is unavoidable (Figure 2D). Approximately 19.41% of Ti, 50.54% of O, 19.84% of C, and 0.84% of N were observed in an NT sample. The occurrence of nitrogen can be ascribed to having been derived from the ammonia fluoride in the electrolyte used to anodize the samples (Figure 2C). Approximately 65.81% of C (59.40% of C in the TET) and 5.55% of N were observed in an NT-T sample. As shown in Figure 2B, the PT and NT substrates show only one peak approximately 529 eV, while the NT-T substrate shows a new peak approximately 533 eV with significant suppression of
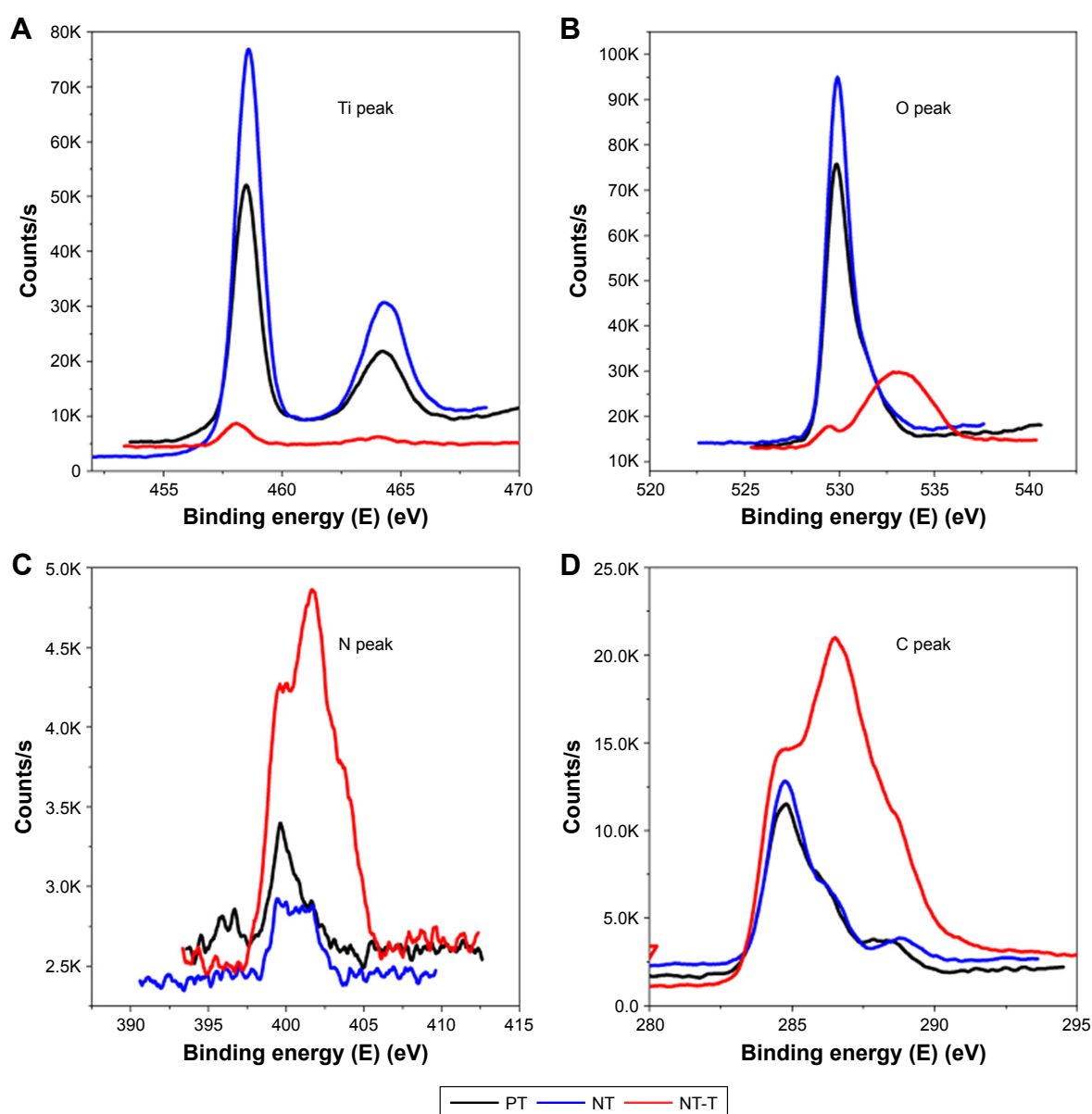
Figure 2 The XPS patterns of the PT, NT, NT-T substrates: (**A**) Ti, (**B**) O, (**C**) N, and (**D**) C.
Abbreviations: NT, nanotubes; NT-T, tetracycline-loaded nanotubes; PT, pure titanium; XPS, X-ray photoelectron spectroscopy.

the peak approximately 529 eV. In the PT and NT substrates, the oxygen valence state should be −2, while the oxygen in the TET is from a C–O covalent bond. This explains the origin of the different peak positions for oxygen in the XPS results. A sharp increase in carbon (Figure 2C) and nitrogen (Figure 2D) content was derived with successful TET loading. These results suggested that TET was deposited into TiO$_2$ nanotubes successfully.

To further confirm the successful loading of NT-T samples, the hydrophilic capability of different samples was characterized with water contact angle measurements (Figure 3). The PT substrates showed contact angles of approximately 77.45°±9.45° (n=3), which were similar to what has been observed in previous studies.[31,33] Consistent with previous studies,[34,35] the NT substrates displayed hydrophilic properties with contact angles of approximately 36.15°±11.67° (n=3). After TET had been deposited, the water contact angles of NT-T samples increased to approximately 38.85°±7.76° (n=3). Furthermore, when compared with PT, the reduction of contact angles in NT and NT-T was significant. The result suggests that NT-T was successfully fabricated.

TET release

The drug loading and release characteristics of the nanotubes to prevent bacterial adhesion were investigated to explore the feasibility of using NT-T substrates as a drug carrier for local therapeutic effects in a surrounding environment. Figure 4 shows the fraction release profiles of TET from
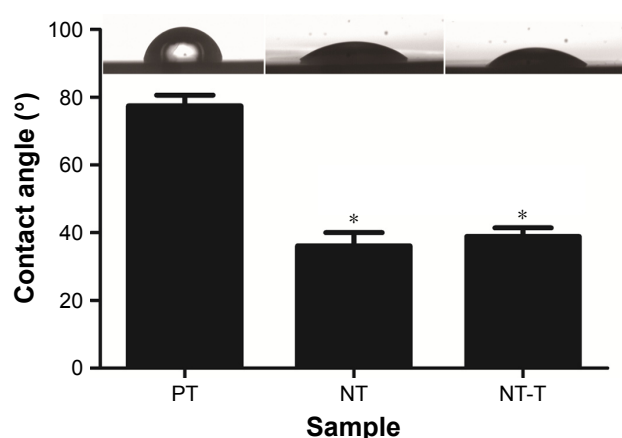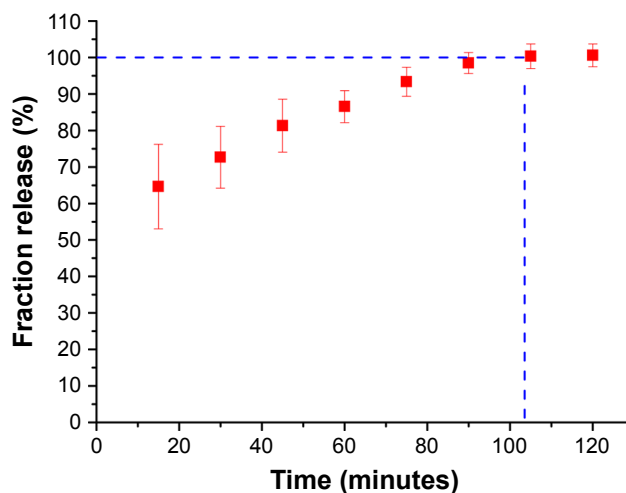
Figure 4 The fraction release of tetracycline from NT-T substrates in vitro (n=3).
Abbreviation: NT-T, tetracycline-loaded nanotubes.

NT-T samples. Approximately 64.24% of TET was released from NT-T after incubation for an initial 15 minutes; the possible reasons for the sudden release of TET is that the binding of TET present in the outermost layer of TiO$_2$ nanotubes was relatively loose, or some TET molecules did not bind but existed inside the molecular voids. After 90 minutes, the TET release curve tended to be stable. The result indicates that TET was partially deposited into the wells of TiO$_2$ nanotubes arrays (NT-T). The result is of great significance for further study of functional titanium-based implants with antibacterial abilities.

Bacterial adhesion

The antibacterial properties of the substrates were characterized using *P. gingivalis*. *P. gingivalis* is a nonglycolytic gram-negative anaerobe that is one of the most potent and well-documented pathogens associated with periodontal disease and is widely used for antibacterial assays. Bacterial adhesion on the surfaces of the PT, NT, and NT-T were surveyed using SEM and fluorescence microscopy for a period of 3 hours. In this research, we evaluated *P. gingivalis* by SEM and fluorescence microscopy.

As shown in the SEM images in Figure 5, there was only a small amount of single bacterial colonies scattered on the surfaces of NT-T for 3 hours, and disintegrating bacteria splints can be seen (Figure 5Ac). There were more bacterial colonies on the NT surfaces than on the NT-T surface after 3 hours (Figure 5Ab). Compared with the NT and NT-T surfaces, multiple bacterial colonies formed colony masses on the PT surfaces during the 3 hours used to survey the
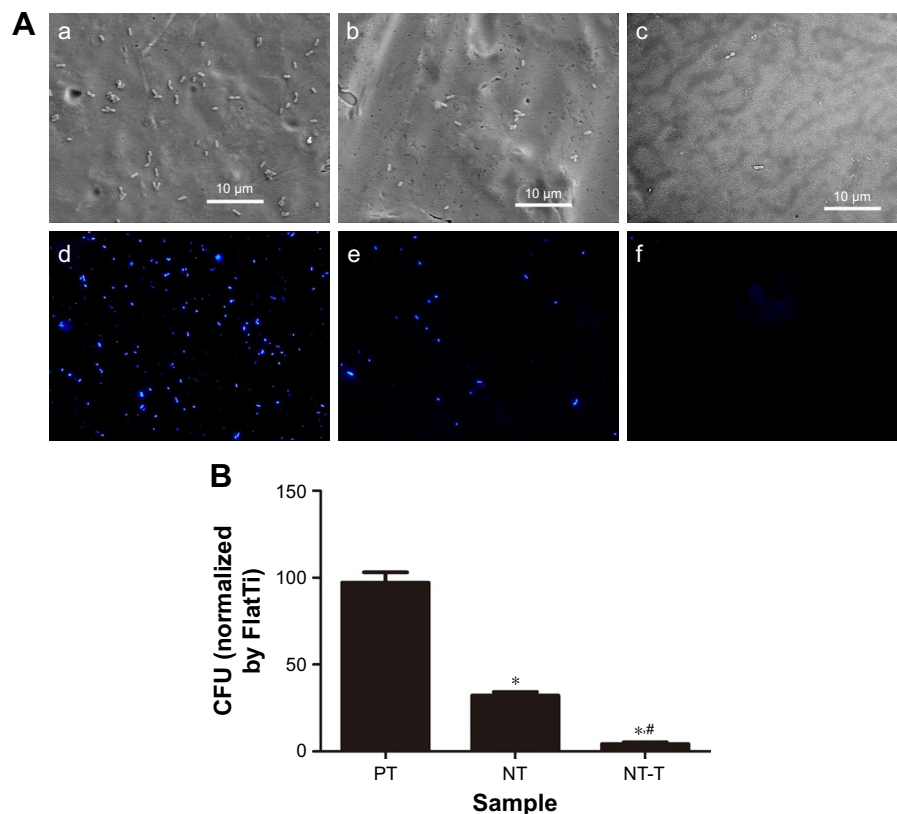
Figure 3 The surface contact angles and water drop profiles of the PT, NT, and NT-T substrates.
Notes: The contact angle is expressed as a measure of hydrophilicity of different substrates. The error bars represent means ± SD (n=3). *A significant difference compared with PT (*P*<0.05).
Abbreviations: NT, nanotubes; NT-T, tetracycline-loaded nanotubes; PT, pure titanium.

Figure 5 Evaluation of antimicrobial activity of different substrates for 3 hours.
Notes: (**A**) SEM of bacterial adhesion on the surfaces of the PT, NT, and NT-T for 3 hours (a–c); Fluorescence microscope images of bacterial colonies adhered on the PT, NT, and NT-T (d–f). (**B**) Bacterial CFU from different substrates for 3 hours. The error bars represent means ± SD (n=3). *A significant difference compared with PT (*P*<0.05). #A significant difference compared with NT (*P*<0.05).
Abbreviations: CFU, colony-forming units; NT, nanotubes; NT-T, tetracycline-loaded nanotubes; PT, pure titanium; SEM, scanning electronic microscopy.

materials (Figure 5Aa). Additionally, as seen in Figure 5B, there were significantly fewer bacterial colonies in the NT and NT-T groups compared with the PT group; moreover, when compared with the NT group, there were significantly fewer bacterial colonies in the NT-T groups during the 3 hours used to survey each sample.

In the fluorescence microscopy images in Figure 5A(d–f), the PT surface has a strong fluorescence intensity. The NT surface's fluorescence intensity was weaker compared with the PT surfaces. Formation of bacterial colonies on the NT-T surface was sparse. This result is consistent with the results obtained from SEM imaging. The above results indicated that the deposition of TET mainly contributed to the antibacterial effects of the material.

Cell adhesion, proliferation, and differentiation

Figure 6A–C shows SEM images of morphologies of different samples cocultured with BMSCs for 120 minutes. The BMSCs grown onto NT substrates (Figure 6B) displayed more cell spreading than those adhered to the PT

samples (Figure 6A). BMSCs cocultured with NT-T samples (Figure 6C) exhibited similar cell spreading compared with those cells that were grown onto NT samples (Figure 6B). More BMSCs were observed on NT and NT-T samples than those in PT samples, whereas the number of BMSCs in NT and NT-T substrates was similar. These results suggest that deposited TET has no adverse effect on BMSCs' adhesion.

An MTT assay was performed for evaluating the cytocompatibility to assess the behavior of substrates that were cocultured with BMSCs. The production of formazan is a by-product of deoxidation formed by viable cells, thus indirectly indicating cellular proliferation. Figure 6D shows the absorbance of formazan, measured using a spectrophotometer, that is produced by BMSCs that have adhered to different samples. After BMSCs were cultured for 1 day, no prominent difference was observed in cell proliferation between all these groups. After culturing for 3 days, BMSCs grown onto NT and NT-T samples exhibited prominently higher cell proliferation than those in PT samples (*P*<0.05). However, no significant difference in cell proliferation was observed between NT and
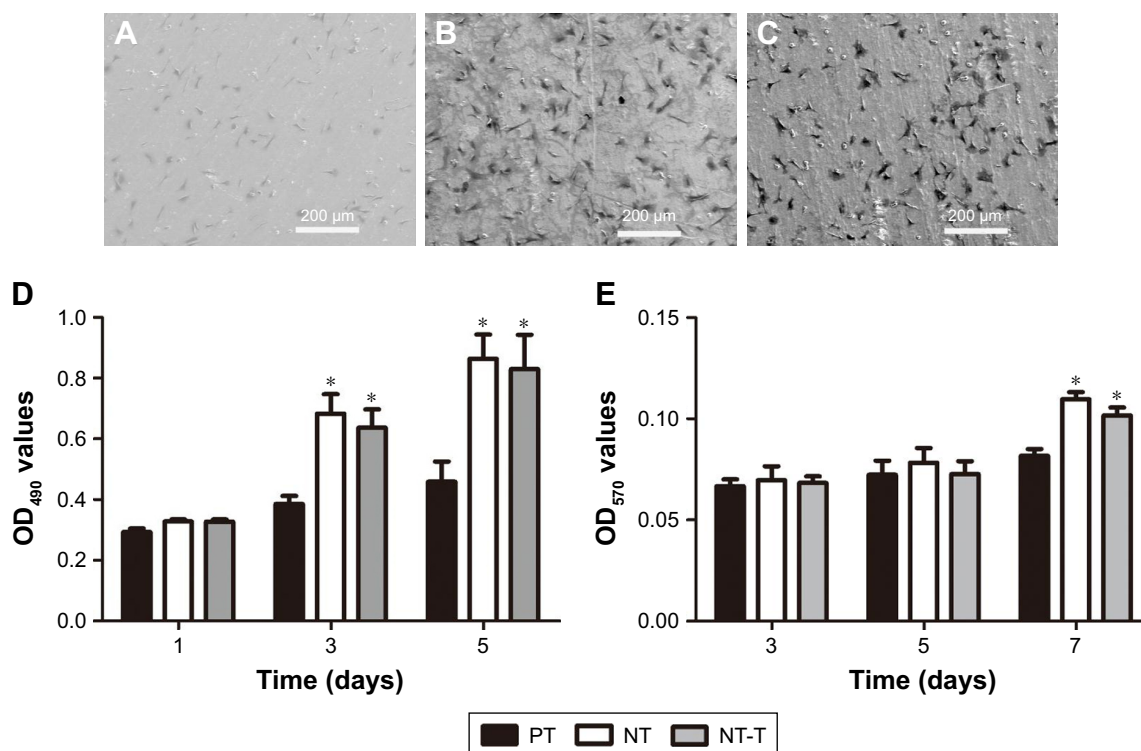
Figure 6 BMSCs on the substrates.
Notes: (**A–C**) The comparison of bacterial colonies adhered on the PT, NT, and NT-T at the 48-hour point. (**D**) MTT assay. Formazan absorbance expressed as a measure of cell proliferation from BMSCs cultured on different substrates for 1, 3, and 5 days. (**E**) Alkaline phosphatase activity of BMSCs cultured on different substrates for 3, 5, and 7 days. The error bars represent means ± SD (n=3). *A significant difference compared with PT ($P<0.05$).
Abbreviations: BMSCs, bone marrow stromal cells; NT, nanotubes; NT-T, tetracycline-loaded nanotubes; PT, pure titanium.

NT-T samples. The results of cell proliferation adherence on different substrates at 5 days of growth were similar to those results observed at 3 days of growth.

The ALP activity was measured after culture for 3, 5, and 7 days (Figure 6E) to investigate the behavior of different samples cocultured with BMSCs on differentiation. After BMSCs were cultured for 3 and 5 days, all groups showed no significant differences. The absorbance representing ALP activity in the NT and NT-T substrates was significantly higher ($P<0.05$) than the absorbance from the PT samples after 7 days of culture. However, no significant difference in ALP activity was observed between NT and NT-T substrates. The expression of ALP activity is an early marker for osteogenesis, which is related to the bone formation and bone matrix mineralization in skeletal tissues. These results suggest that TET loading in TiO_2 nanotubes has no adverse effect on the adhesion, proliferation, and differentiation of BMSCs, and NT-T substrates were beneficial for these properties in BMSCs.

Conclusions

In this study, we prepared NT and NT-T specimens successfully. Antibacterial experiments in vitro revealed that

the NT surface had antibacterial properties; meanwhile, the NT-T surface had increased antibacterial properties. The results from TET loading showed that TET could be deposited onto TiO_2 nanotubes. The TET release curve was also explored. We also studied the cocultivation of BMSCs with specimens. The results showed that NT and NT-T specimens' surface could also promote the biological activities of BMSCs. In summary, TET-loaded TiO_2 nanotubes have the potential to be applied to develop titanium implants with antibacterial properties.

Acknowledgment

Disclosure

The authors report no conflicts of interest in this work.

References

1. Hanawa T. Materials for metallic stents. *J Artif Organs*. 2009;12(2): 73–79.
2. Ananth H, Kundapur V, Mohammed HS, Anand M, Amarnath GS, Mankar S. A review on biomaterials in dental implantology. *Int J Biomed Sci*. 2015;11(3):113–120.

3. Wassmann T, Kreis S, Behr M, Buergers R. The influence of surface texture and wettability on initial bacterial adhesion on titanium and zirconium oxide dental implants. *Int J Implant Dent*. 2017;3(1):32.

4. de Avila ED, Vergani CE, Mollo Junior FA, Junior MJ, Shi W, Lux R. Effect of titanium and zirconia dental implant abutments on a cultivable polymicrobial saliva community. *J Prosthet Dent*. 2017;118(4):481–487.

5. Zaatreh S, Haffner D, Strauss M, et al. Thin magnesium layer confirmed as an antibacterial and biocompatible implant coating in a co-culture model. *Mol Med Rep*. 2017;15(4):1624–1630.

6. Kolenbrander PE, Palmer RJ, Periasamy S, Jakubovics NS. Oral multispecies biofilm development and the key role of cell-cell distance. *Nat Rev Microbiol*. 2010;8(7):471–480.

7. Lindhe J, Meyle J, Group D of European Workshop on Periodontology. Peri-implant diseases: Consensus Report of the Sixth European Workshop on Periodontology. *J Clin Periodontol*. 2008; 35(8 Suppl):282–285.

8. Lang NP, Bosshardt DD, Lulic M. Do mucositis lesions around implants differ from gingivitis lesions around teeth? *J Clin Periodontol*. 2011;38(Suppl 11):182–187.

9. Heitz-Mayfield LJ. Peri-implant diseases: diagnosis and risk indicators. *J Clin Periodontol*. 2008;35(8 Suppl):292–304.

10. Zitzmann NU, Berglundh T. Definition and prevalence of peri-implant diseases. *J Clin Periodontol*. 2008;35(8 Suppl):286–291.

11. Pye AD, Lockhart DE, Dawson MP, Murray CA, Smith AJ. A review of dental implants and infection. *J Hosp Infect*. 2009;72(2): 104–110.

12. Heydenrijk K, Meijer HJ, van der Reijden WA, Raghoebar GM, Vissink A, Stegenga B. Microbiota around root-form endosseous implants: a review of the literature. *Int J Oral Maxillofac Implants*. 2002; 17(6):829–838.

13. Moslemi N, Shahnaz A, Bahador A, Torabi S, Jabbari S, Oskouei ZA. Effect of postoperative amoxicillin on early bacterial colonization of peri-implant sulcus: a randomized controlled clinical trial. *J Dent*. 2016;13(5):309–317.

14. Park J, Tennant M, Walsh LJ, Kruger E. Is there a consensus on antibiotic usage for dental implant placement in healthy patients? *Aust Dent J*. 2018;63(1):25–33.

15. Mainjot A, D'Hoore W, Vanheusden A, van Nieuwenhuysen JP. Antibiotic prescribing in dental practice in Belgium. *Int Endod J*. 2009; 42(12):1112–1117.

16. Lewis MA. Why we must reduce dental prescription of antibiotics: European Union Antibiotic Awareness Day. *Br Dent J*. 2008;205(10): 537–538.

17. Lin WT, Tan HL, Duan ZL, et al. Inhibited bacterial biofilm formation and improved osteogenic activity on gentamicin-loaded titania nanotubes with various diameters. *Int J Nanomedicine*. 2014;9:1215–1230.

18. Yeniyol S, He Z, Yüksel B, et al. Antibacterial activity of as-annealed TiO₂ nanotubes doped with Ag nanoparticles against periodontal pathogens. *Bioinorg Chem Appl*. 2014;2014:829496–829498.

19. Popat KC, Eltgroth M, Latempa TJ, Grimes CA, Desai TA. Decreased *Staphylococcus* epidermis adhesion and increased osteoblast functionality on antibiotic-loaded titania nanotubes. *Biomaterials*. 2007; 28(32):4880–4888.

20. Nguyen F, Starosta AL, Arenz S, Sohmen D, Dönhöfer A, Wilson DN. Tetracycline antibiotics and resistance mechanisms. *Biol Chem*. 2014; 395(5):559–575.

21. Hu X, Meng G, Huang Q, et al. Large-scale homogeneously distributed Ag-NPs with sub-10 nm gaps assembled on a two-layered honeycomb-like TiO₂ film as sensitive and reproducible SERS substrates. *Nanotechnology*. 2012;23(38):385705.

22. Ariani MD, Matsuura A, Hirata I, Kubo T, Kato K, Akagawa Y. New development of carbonate apatite-chitosan scaffold based on lyophilization technique for bone tissue engineering. *Dent Mater J*. 2013;32(2):317–325.

23. Chow SF, Wan KY, Cheng KK, et al. Development of highly stabilized curcumin nanoparticles by flash nanoprecipitation and lyophilization. *Eur J Pharm Biopharm*. 2015;94:436–449.

24. Sherertz RJ, Raad II, Belani A, et al. Three-year experience with sonicated vascular catheter cultures in a clinical microbiology laboratory. *J Clin Microbiol*. 1990;28(1):76–82.

25. Bjerkan G, Witsø E, Bergh K. Sonication is superior to scraping for retrieval of bacteria in biofilm on titanium and steel surfaces in vitro. *Acta Orthop*. 2009;80(2):245–250.

26. Xu D, Yang W, Hu Y, et al. Surface functionalization of titanium substrates with cecropin B to improve their cytocompatibility and reduce inflammation responses. *Colloids Surf B Biointerfaces*. 2013; 110:225–235.

27. Sopha H, Samoril T, Palesch E, et al. Ideally hexagonally ordered TiO₂ nanotube arrays. *ChemistryOpen*. 2017;6(4):480–483.

28. Aguirre R, Echeverry-Rendón M, Quintero D, et al. Formation of nanotubular TiO₂ structures with varied surface characteristics for biomaterial applications. *J Biomed Mater Res A*. 2018;106(5):1341–1354.

29. Khudhair D, Amani Hamedani H, Gaburro J, et al. Enhancement of electro-chemical properties of TiO₂ nanotubes for biological interfacing. *Mater Sci Eng C Mater Biol Appl*. 2017;77:111–120.

30. Liu P, Zhao Y, Yuan Z, et al. Construction of Zn-incorporated multilayer films to promote osteoblasts growth and reduce bacterial adhesion. *Mater Sci Eng C Mater Biol Appl*. 2017;75:998–1005.

31. Xu D, Yang W, Hu Y, et al. Surface functionalization of titanium substrates with cecropin B to improve their cytocompatibility and reduce inflammation responses. *Colloids Surf B Biointerfaces*. 2013; 110:225–235.

32. Cai K, Lai M, Yang W, et al. Surface engineering of titanium with potassium hydroxide and its effects on the growth behavior of mesenchymal stem cells. *Acta Biomater*. 2010;6(6):2314–2321.

33. Hu Y, Cai K, Luo Z, Jandt KD. Layer-by-layer assembly of β-estradiol loaded mesoporous silica nanoparticles on titanium substrates and its implication for bone homeostasis. *Adv Mater*. 2010;22(37): 4146–4150.

34. Peng Z, Ni J, Zheng K, et al. Dual effects and mechanism of TiO₂ nanotube arrays in reducing bacterial colonization and enhancing C3H10T1/2 cell adhesion. *Int J Nanomedicine*. 2013;8:3093–3105.

35. Yang L, Zhang M, Shi S, et al. Effect of annealing temperature on wettability of TiO2 nanotube array films. *Nanoscale Res Lett*. 2014; 9(1):621.